Offset-frequency locking of extended-cavity diode lasers for precision spectroscopy of water at 1.38 μm

A. Castrillo[1], E. Fasci[1], G. Galzerano[2], G. Casa[1], P. Laporta[2], and L. Gianfrani[1,*]

[1]*Dipartimento di Scienze Ambientali della Seconda Università di Napoli, and CNISM - Unità Napoli 2, Via Vivaldi 43, 81100 Caserta, Italy*

[2]*Istituto di Fotonica e Nanotecnologie - CNR and Dipartimento di Fisica del Politecnico di Milano, Piazza Leonardo Da Vinci 32, 20133 Milano, Italy*

[*]*livio.gianfrani@unina2.it*

Abstract: We describe a continuous-wave diode laser spectrometer for water-vapour precision spectroscopy at 1.38 μm. The spectrometer is based upon the use of a simple scheme for offset-frequency locking of a pair of extended-cavity diode lasers that allows to achieve high levels of accuracy and reproducibility in measuring molecular absorption. When locked to the master laser with an offset frequency of 1.5 GHz, the slave laser exhibits residual frequency fluctuations of $\sim$ 1 kHz over a time interval of 25 minutes, for a 1-s integration time. The slave laser could be continuously tuned up to 3 GHz, the scan showing relative deviations from linearity below the 10^{-6} level. Simultaneously, a capture range of the order of 1 GHz was obtained. Quantitative spectroscopy was also demonstrated by accurately determining relevant spectroscopic parameters for the $2_{2,1}\rightarrow 2_{2,0}$ line of the $H_2{}^{18}O$ $\nu_1+\nu_3$ band at 1384.6008 nm.

OCIS codes: (140.3425) Laser stabilization; (300.6260) Spectroscopy, diode lasers; (300.6390) Spectroscopy, molecular.

References and links

1. L. Cacciapuoti, M. de Angelis, M. Fattori, G. Lamporesi, T. Petelski, M. Prevedelli, J. Stuhler, and G. M. Tino, "Analog+digital phase and frequency detector for phase docking of diode lasers," Rev. Sci. Instrum. **76,** 053111 (2005).
2. U. Schünemann, H. Engler, R. Grimm, M. Weidemüller, and M. Zielonkowski, "Simple scheme for tunable frequency offset locking of two lasers," Rev. Sci. Instrum. **70,** 242-243 (1999).
3. T. Stace, A. N. Luiten, and R. P. Kovacich, "Laser offset-frequency locking using a frequency-to-voltage converter," Meas. Sci. Technol. **9,** 1635-1637 (1998).
4. G. Ritt, G. Cennini, C. Geckeler, M. Weitz "Laser frequency offset locking using a side of filter technique," Appl. Phys. B **79,** 363-365 (2004).
5. S. Schilt, R. Matthey, D. Kauffmann-Werner, C. Affolderbach, G. Mileti, and L. Thévenaz, "Laser offset-frequency locking up to 20 GHz using a low-frequency electrical filter technique," Appl. Opt. **47,** 4336-4344 (2008).
6. J. Hughes and C. Fertig, "A widely tunable laser frequency offset lock with digital counting," Rev. Sci. Instrum. **79,** 103104 (2008).
7. G. Casa, A. Castrillo, G. Galzerano, R. Wehr, A. Merlone, D. Di Serafino, P. Laporta, and L. Gianfrani, "Primary gas thermometry by means of laser absorption spectroscopy: Determination of the Boltzmann constant," Phys. Rev. Lett. **100,** 200801 (2008).

#132562 - $15.00 USD Received 30 Jul 2010; revised 23 Sep 2010; accepted 23 Sep 2010; published 29 Sep 2010

8. A. Castrillo, G. Casa, A. Merlone, G. Galzerano, P. Laporta, and L. Gianfrani, "On the determination of the Boltzmann constant by means of precision molecular spectroscopy in the near-infrared," C. R. Physique **10,** 894-906 (2009).
9. G. Galzerano, E. Fasci, A. Castrillo, N. Coluccelli, L. Gianfrani, and P. Laporta, "Absolute frequency stabilization of an extended-cavity diode laser against Doppler-free $H_2{}^{17}O$ absorption lines at 1.384 μm," Opt. Lett. **34,** 3107-3110 (2009).
10. G. Galzerano, A. Gambetta, E. Fasci, A. Castrillo, M. Marangoni, P. Laporta, and L. Gianfrani, "Absolute frequency measurement of a waterstabilized diode laser at 1.384 μm by means of a fiber frequency comb," Appl. Phys. B, in press.
11. A. Merlone, F. Moro, A. Castrillo, and L. Gianfrani, "Design and capabilities of the temperature control system for the Italian experiment based upon precision laser spectroscopy for a new determination of the Boltzmann constant," Int. J. Thermophys., in press.
12. R. Ciurylo, "Shape of pressure- and Doppler-broadened spectral lines in the core and near wings," Phys. Rev. A **58,** 1029-1039 (1998).
13. A. Gambetta, E. Fasci, A. Castrillo, M. Marangoni, G. Galzerano, G. Casa, P. Laporta, and L. Gianfrani, "Frequency metrology in the near-infrared spectrum of $H_2{}^{17}O$ and $H_2{}^{18}O$ molecules: Testing a new inversion method for energy levels retrieval," New J. Physics, in press.
14. L. S. Rothman, I. E. Gordon, A. Barbe, D.Chris Benner, P. F. Bernath, M. Birk, V. Boudon, L. R. Brown, A. Campargue, J.-P. Champion, K. Chance, L. H. Coudert, V. Dana, V. M. Devi, S. Fally, J.-M. Flaud, R. R. Gamache, A. Goldman, D. Jacquemart, I. Kleiner, N. Lacome, W.J. Lafferty, J.-Y. Mandin, S. T. Massie, S.N. Mikhailenko, C. E. Miller, N. Moazzen-Ahmadi, O. V. Naumenko, A.V. Nikitin, J. Orphal, V.I. Perevalov, A. Perrin, A. Predoi-Cross, C. P. Rinsland, M. Rotger, M. Ŝimecková, M. A. H. Smith, K. Sung, S. A. Tashkun, J. Tennyson, R. A. Toth, A. C. Vandaele, and J. Vander Auwera, " The HITRAN 2008 molecular spectroscopic database," J. Quant. Spectr. Rad. Transf. **110,** 533-572 (2009).
15. B. E. Grossmann and E. V. Browell, "Spectroscopy of water vapor in the 720-nm wavelength region: Line strengths, self-induced pressure broadenings and shifts, and temperature dependence of linewidths and shifts," J. Mol. Spectrosc. **136,** 264-294 (1989).
16. K. Iwata and Y. Kusumoto, "Modification of Takaishi-Sensui formula for a diaphragm gauge system connected by an arbitrary length pipe," Vacuum **84,** 729-733 (2010).
17. H. W. Yoon, J. J. Butler, T. C. Larason, and G. P. Eppeldauer, "Linearity of InGaAs photodiodes," Metrologia **40,** S154-S158 (2003).
18. C. Daussy, M. Guinet, A. Amy-Klein, K. Djerroud, Y. Hermier, S. Briaudeau, Ch. J. Bordé, and C. Chardonnet, "Direct Determination of the Boltzmann Constant by an Optical Method," Phys. Rev. Lett. **98,** 250801 (2008).

1. Introduction

Precise control, stabilization and synchronization of laser frequencies are required in many research applications, including time and frequency metrology, as well as high resolution atomic and molecular spectroscopy. Such a demanding goal can be achieved by means of optical phase-locking techniques, which are often implemented even being very complicated, especially when semiconductor diode lasers are used, because of their relatively wide emission width. There are typically two approaches for building an optical phase-locked-loop (OPLL): one is based upon analog phase detectors, the other employs digital phase and frequency detectors. Recently, the best performances in terms of noise, bandwidth, robustness and reliability have been demonstrated when using both approaches in a mutually exclusive way [1]. However, there are several applications in which it is unnecessary to make use of an OPLL. In particular, phase coherency is not required in many spectroscopic experiments, whereas it is sufficient that the probing laser (named slave laser) maintains a highly-precise frequency-offset from a reference laser (usually referred to as master laser). In this case, it is possible to implement simple locking schemes, while ensuring high frequency stability and accuracy. In these schemes, the reference laser is frequency stabilized against a molecular or atomic line and a beat note between the two lasers is usually generated. Hence, the frequency of the beat note is locked to a constant value by using a servo system acting on the slave laser. The main difference between offset-frequency locking methods, which have been developed in the last decade, usually consists in the way the error signal is generated. Schünemann et al. used an electronic delay line as frequency-dependent phase shifter in conjunction to a standard phase detector [2]. This simple scheme

#132562 - $15.00 USD Received 30 Jul 2010; revised 23 Sep 2010; accepted 23 Sep 2010; published 29 Sep 2010

has the disadvantage of multiple locking points. Moreover, the length of the delay line is a critical parameter, influencing in opposite ways two key features: the slope of the error signal and the capture range. Therefore, a trade-off is necessary since an increased length would result in a larger slope but in a reduced capture range. A radically different approach makes use of a frequency-to-voltage converter, whose output voltage is compared to a reference voltage, thus setting the offset-frequency [3]. This method offers the advantage of being very efficient in reducing inter-laser frequency instabilities, but has the drawback of a limited operating frequency, typically smaller than 1 MHz, as determined by the bandwidth of the frequency-to-voltage converter. Offset-locking at high frequencies (of the order of several GHz) has been demonstrated using the amplitude response of a sharp electronic RF high-pass filter [4]. An alternative to this method, based on a frequency modulation added to one of the lasers, has been reported very recently [5]. Hence, the joint use of a low-bandwidth electrical filter, an envelope detector and a lock-in amplifier produces an error signal that is used for the locking purpose. Expressly designed for LIDAR applications, this latter system ensures offset-frequency locking up to 20 GHz, but the slope of the dispersion signal is not sufficiently high to provide the stability performance that is required in precision spectroscopy.

In the large majority of schemes for offset-frequency locking, the beat note is down shifted by heterodyne mixing with the output of a radio frequency synthesizer (or a voltage controlled oscillator) and properly processed by analog electronics. Alternatively, the shifted AC signal can be directly counted by means of fast digital electronics, converted into a voltage by using a digital-to-analog converter and subsequently compared to a set-point voltage in order to produce an analog error signal [6]. Such a hybrid system ensures a wide tuning range and a high stability level, but surely adds some complexity.

So far, atomic spectroscopy has largely benefited of the technologies of which we have provided an overview, mostly for applications to cold atoms manipulation involving the visible and near-infrared spectrum of alkali atoms. Nowadays, the transfer of these and other sophisticated techniques is being performed towards molecular physics, mostly stimulated by the recent progress in the field of cold molecules. In this paper, we report on the development and test of an absorption spectrometer based upon a pair of offset-frequency locked extended-cavity diode lasers, expressly designed for applications to precision spectroscopy of water vapour at 1.38 μm. We implemented a simple and robust offset-frequency locking scheme characterized by high stability, wide versatility and strong reliability, using an analog phase/frequency detector. The system performance was deeply investigated, mainly in view of its use for a spectroscopic determination of the Boltzmann constant [7, 8].

2. Experimental apparatus

Figure 1 reports the block diagram of the offset-locking scheme. The beat note between two extended cavity diode lasers, provided by a 12-GHz bandwidth photodetector (New Focus 1567-A), is first amplified by $\sim$20 dB (RF Bay LPA-8-17) and subsequently scaled in frequency by a factor of 10 using a high-speed divider (RF Bay FPS-10-12). Hence, a power splitter (RF Bay PSC-2-6) produces a monitor signal, while its main output signal is sent to a phase/frequency detector with a frequency range of 3-300 MHz (RF Bay PDF-100), which compares it to a reference signal provided by a RF synthesizer (Rohde & Schwarz SML01) thus producing an error signal. This latter is properly integrated and used to continuously lock the frequency of the beat note with that of the reference signal. To this purpose, a double-servo system acts on the diode injection current and on the extended-cavity length (by means of a piezoelectric transducer) and allows to actively control the emission frequency of one of the two lasers, i.e. the slave laser (SL), so that to maintain a constant frequency offset between SL and the other laser, namely the master laser (ML). The control loop bandwidth was found to be $\sim$10 kHz, limited by the output

#132562 - $15.00 USD Received 30 Jul 2010; revised 23 Sep 2010; accepted 23 Sep 2010; published 29 Sep 2010

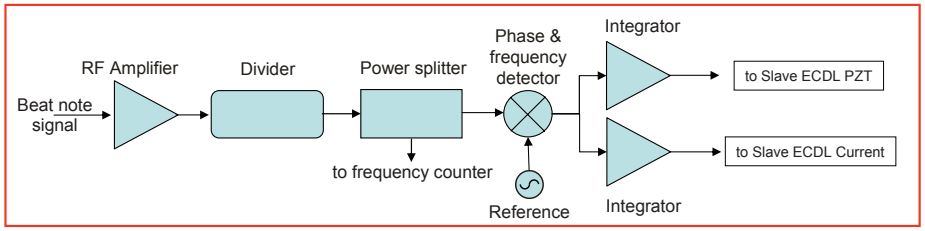

Fig. 1. Block diagram of the offset-locking electronics.

dynamics of the phase/frequency detector. By tuning the frequency of the reference signal, it is possible to perform continuous and highly-accurate frequency scans of the SL. In the present configuration, the offset frequency can be continuously tuned between 100 MHz and 3 GHz, with any step between 0.1 and 500 MHz. Of course, the maximum offset frequency could be increased by using a higher order frequency divider.

Figure 2 shows the schematics of the spectrometer, which was used to perform a complete characterization of the offset-locking technique. The master laser, already described elsewhere, presents an emission linewidth of $\sim$30 kHz and a sub-kilohertz absolute stabilization of its central frequency [9]. Very briefly, this high performance is reached by locking the frequency against a saturated absorption line of the $H_2{}^{17}O$ molecule at 1384.5919 nm. The non-linear regime of laser-gas interaction is achieved by filling a high-finesse optical resonator with $H_2{}^{17}O$ at low pressure. The laser frequency is locked to the resonator by means of the Pound-Drever-Hall technique, as illustrated in Fig. 2. Hence, the cavity mode frequency is locked to the center of the Lamb-dip, which is detected by using a wavelength modulation method. To this purpose, the cavity resonance is dithered by means of a sinusoidal signal at 2 kHz, while a lock-in amplifier performs a synchronous processing of the cavity transmitted signal, thus allowing to retrieve an error signal given by the first derivative of the Lamb-dip. Such a signal, once properly integrated, is used to actively control the cavity length. As a result of an Allan variance analysis of the beat frequency between the water-stabilized laser and the nearest tooth of a self-referenced fiber-comb, a relative frequency stability of the order of 10^{-12} for an integration time of 100 s was measured, mostly limited by the frequency noise of the GPS-disciplined Rb microwave clock that was employed for the stabilization of the carrier-envelope-offset frequency and of the repetition rate of the fiber comb [10]. Operating in a Littrow configuration, the slave laser emits on a single mode with a typical output power of about 2 mW. An optical isolator is used to prevent undesired backreflections, which might disturb the operation of the SL. An acousto-optic modulator (AOM) allows to deflect from the primary beam to the first diffracted order about 50% of the available laser power. Driven by a 0.5-W radio frequency signal at 80 MHz, the AOM serves as an actuator within a servo loop in order to keep constant the power of the laser beam that is used for the spectroscopic experiment. A portion of the SL beam is perfectly overlapped with a portion of the ML beam. Hence, the two co-propagating beams are focused on the fast InGaAs photodetector that provides the beat note between the two lasers. The remaining portion of the SL beam passes through an isothermal cell containing a water vapour

#132562 - $15.00 USD Received 30 Jul 2010; revised 23 Sep 2010; accepted 23 Sep 2010; published 29 Sep 2010

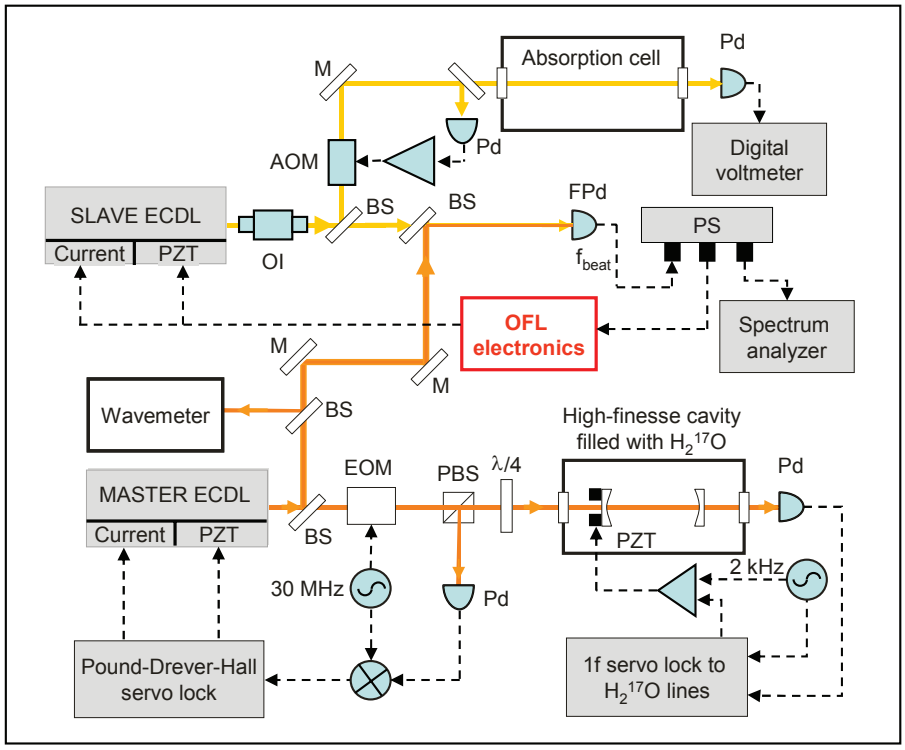

Fig. 2. Schematic diagram of the dual-laser absorption spectrometer. OI: optical isolator; BS: beam splitter; AOM: acousto-optic modulator; EOM: electro-optic phase modulator; $\lambda/4$: quarter wave plate; M: mirror; PZT: piezoelectric transducer; PBS: polarizing beam splitter; Pd: photodiode; FPd: fast photodiode; PS: RF power-splitter; OFL: offset-frequency locking.

sample. Equipped with a pair of antireflection-coated BK7 windows, the isothermal cell is 150-mm long and it is referenced to the triple point of water (TPW), with temperature accuracy, uniformity and stability at the level of 0.1 mK, as extensively described elsewhere [11]. A 97% enriched ^{18}O water sample (with a nominal purity better than 99.9%) is used to fill the gas cell at a pressure variable between 1 and 500 Pa, as measured by means of a capacitance pressure gauge (with an accuracy of 0.25% of the reading). The intensity of the laser beam, after a single pass through the cell, is monitored by a pre-amplified InGaAs photodetector, whose output voltage is directly measured by a 6½-digit voltmeter connected to a personal computer through a USB-GPIB board. Other instruments interfaced to the computer are the RF synthesizer and the universal counter. A LabVIEW© code was developed to perform a step-by-step frequency scan and to acquire, for each step, the beat note frequency and the transmitted signal.

3. Results and discussion

Several experiments were performed in order to characterize the performance of the offset-frequency locking scheme. First of all, the stability of the optical beat note was carefully tested

#132562 - $15.00 USD Received 30 Jul 2010; revised 23 Sep 2010; accepted 23 Sep 2010; published 29 Sep 2010

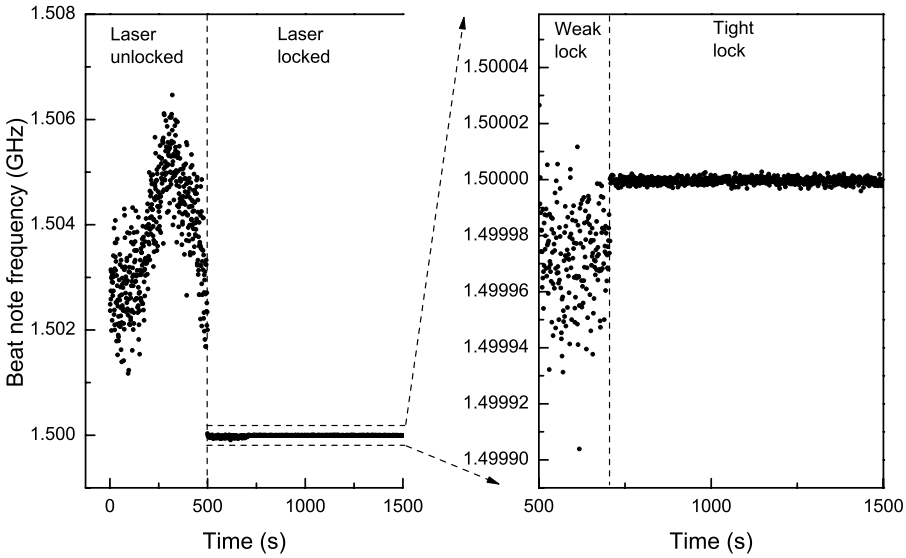

Fig. 3. Beat note frequency versus time for unlocked and offset-frequency locked lasers. A weak lock was activated at 500 s, while a tight lock started operating at 700 s. The offset frequency was set to 1.5 GHz.

by continuously measuring its frequency using a universal counter (Agilent 53131A), with a gate time of 1 s. In fact, the beat note between the two lasers exhibits a signal-to-noise ratio of 40 dB in a 100-kHz resolution bandwidth, which is sufficient for direct counting. The results are reported in Fig. 3, where a weak lock (controlling only the SL extended-cavity length) was activated after the first 500 s of observation, setting the offset frequency at 1.5 GHz. The same figure shows the benefits of a tight lock (acting on both the injection current and the extended-cavity length) that improves the stability by a factor of 15, as compared to the weak lock. Similarly, Fig. 4(a) shows the time behaviour of the beat note over a time span of 25 minutes, evidencing a root-mean-square fluctuation of $\sim$1 kHz, essentially limited by the frequency noise of the slave laser. From this dataset the Allan deviation, σ(y), was calculated for integration times, τ, varying between 1 and 256 s and plotted in Fig. 4(b). In this graph, it is clearly evidenced a trend that can be interpolated by the function $1/\tau^{1/2}$, providing indication of the occurrence of a white-type frequency noise. For integration times longer than 100 s, the relative deviation drops below the 10^{-7} level, thus demonstrating a better stability performance as compared to Refs. 4 and 6. The inset shows the power spectral density of the beat note, observed with a resolution bandwidth of 10 Hz, along with a fit to a Gaussian function that yields a FWHM of $\sim$800 kHz. This value is consistent with the SL emission width, as observed on a time scale of the order of 1 minute.

In order to test the potential of the spectrometer for the highly precise and accurate observation of molecular absorption lineshapes, the slave laser was tuned into resonance with the $2_{2,1}\rightarrow 2_{2,0}$ line of the $H_2{}^{18}O$ $\nu_1+\nu_3$ band at 1384.6008 nm.

In Fig. 5, an example of repeated acquisitions of the absorption profile is shown. These spectra were acquired at a pressure of about 50 Pa and a temperature of 273.1561(2) K, the laser span being 2.55 GHz, obtained with 255 steps of 10 MHz each and a time constant of 100 ms.

#132562 - $15.00 USD Received 30 Jul 2010; revised 23 Sep 2010; accepted 23 Sep 2010; published 29 Sep 2010

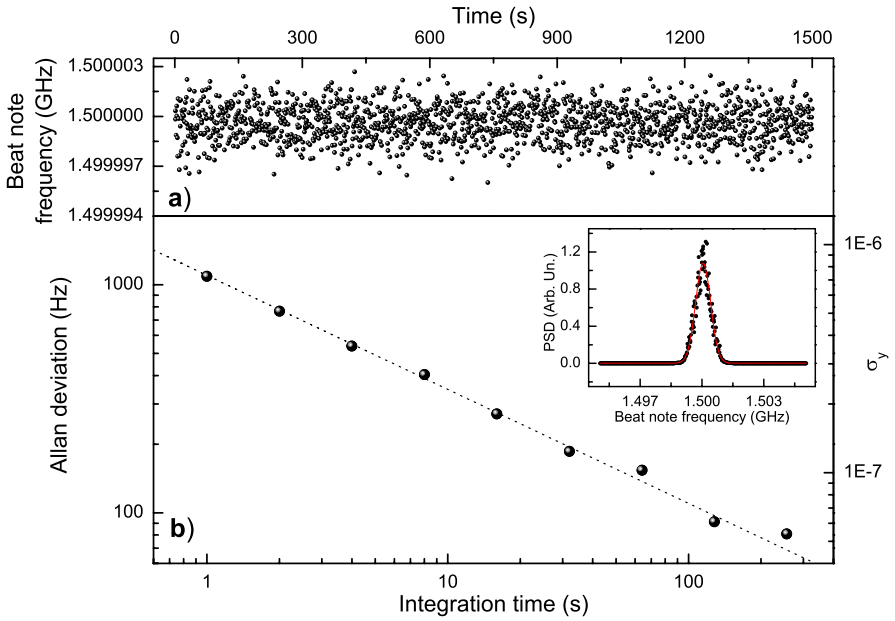

Fig. 4. Plot of the Allan-deviation as a function of the integration time, calculated for the time series reported in the upper part of the figure. The dashed line provides indication of the expected noise reduction for a white-type frequency noise. The inset shows the power spectral density (PSD) of the beat note, along with a fit to a Gaussian function with a FWHM of 800 kHz (red line). The resolution bandwidth was 10 Hz.

The nearly perfect overlapping between the spectra gives a first idea of the high reproducibility level achieved in the present experiment, when making continuous spectra acquisitions over a time interval of about two hours. In the lower part of the figure, the measured beat frequencies, for one of the performed scans, have been reported as a function of the step index, along with a fit to a straight line. The fit residuals (computed as relative deviations between theory and experiment) demonstrate the excellent linearity of the frequency scan, characterized by a linear correlation coefficient differing from 1 by less than 2×10^{-11}. It is worth noting how the fluctuations in the residuals slightly increase by decreasing the frequency separation between the two lasers. This might be due to an instrumental effect and, at least partially, to a slightly worse quality of the offset locking. In fact, the counter can not guarantee the same reproducibility in reading the frequency, since the signal-to-noise ratio of the beat note slightly deteriorates when its frequency approaches the lower limit that is set by the divider (i.e., 100 MHz). Moreover, since the width of the beat note is constant over the full scan, counting precision increases with the frequency separation between the two lasers. Laser scans of 3 GHz were also performed for different values of the frequency steps, up to a maximum of 500 MHz. Similarly, the capture range was found to be close to 1 GHz, by testing the locking capability as a function of the initial frequency separation between the two lasers. At the aim of quantifying the reproducibility of repeated SL scans, line center frequencies were retrieved from the recorded spectra by means of a nonlinear least-squares analysis based on the Levenberg-Marquardt algorithm. As expected, the Voigt model was incapable of fitting the measured spectrum at the present high level of precision and yielded an overly broad profile, as evinced by the clear ”w” structure characterising its residuals. Instead, successful interpolations were carried out by using a Galatry profile, accounting for the occurrence of Dicke narrowing effects [12]. The semiclassical

#132562 - $15.00 USD Received 30 Jul 2010; revised 23 Sep 2010; accepted 23 Sep 2010; published 29 Sep 2010

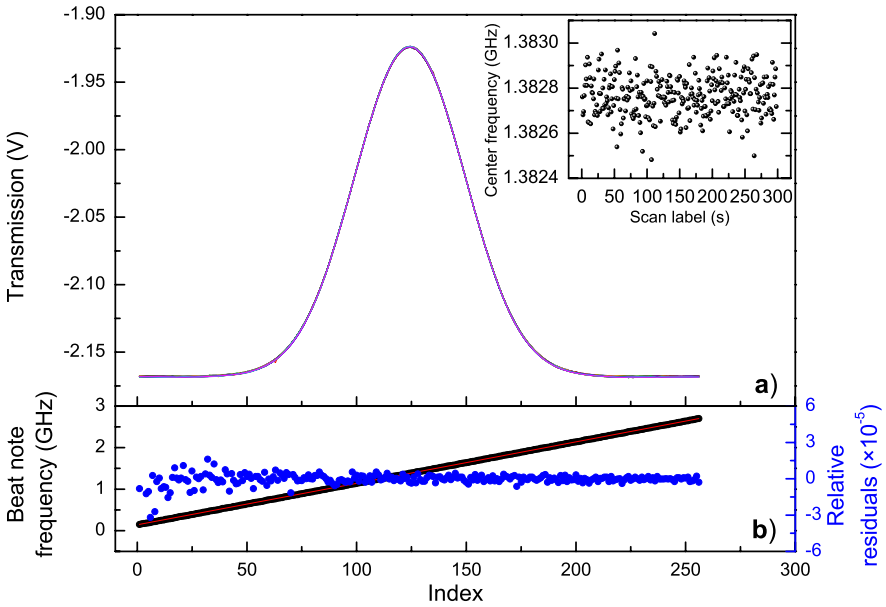

Fig. 5. Example of repeated acquisitions of the absorption profile of the $H_2{}^{18}O$ line at 1384.6008 nm. The set dimension is equal to 300. The lower part reports the plot of the measured frequencies of the beat-note corresponding to one of the consecutive scans of the slave laser. Relative residuals of a fit to a straight line exhibit a root-mean-square value of 4×10^{-6}. In the inset, the center frequency refers to as the shift of the $H_2{}^{18}O$ line center with respect to the ML frequency.

model best reproducing the absorption profile and, hence, capable of describing the physical situation of self-colliding H_2O molecules would be an important issue to be deeply investigated. However, this goes beyond the aim of the present article and will be studied in the near future. The retrieved line center frequencies are reported in the inset of Fig. 5. A 1-σ fluctuation of 87 kHz was measured, corresponding to a stability of $\sim 4 \times 10^{-10}$, as compared to the optical absolute frequency. This fluctuation is significantly larger with respect to that of the beat note, shown in Fig. 4(a). We believe that it is mostly due to the statistical uncertainty in retrieving the line center. Furthermore, any variation of the ML frequency during the overall acquisition time would lead to a change of the SL frequency and therefore should contribute to such a fluctuation, because of the absolute nature of the frequency reference given by the $H_2{}^{18}O$ line. Nevertheless, such a contribution should not exceed the limit of 10 kHz, as indicated be a recent study on the ML absolute stability [13]. It is worth noting that no drift was evidenced in the inset of Fig. 5, further demonstrating the high reproducibility of the dual-laser spectrometer.

As a further test of the potential for quantitative spectroscopy, the integrated absorbance was also retrieved for each of the 300 spectra of Fig. 5. This data set exhibited a relative standard deviation of about 0.3%, mostly due to a small drift towards higher values that could be explained in terms of interaction with the cell walls. In fact, memory effects can not be completely avoided because of the strong electric dipole moment of the water molecule that gives raise to slow adsorption or degassing processes, thus influencing the gas pressure in the medium- and long-term.

By doing absorption spectroscopy as a function of the gas pressure, we could determine the relevant spectroscopic parameters for the selected $H_2{}^{18}O$ line, namely the pressure broadening

#132562 - $15.00 USD Received 30 Jul 2010; revised 23 Sep 2010; accepted 23 Sep 2010; published 29 Sep 2010

Table 1. Measured spectroscopic parameters for the $2_{2,1}\rightarrow 2_{2,0}$ line of the $H_2{}^{18}O$ $\nu_1+\nu_3$ band, at the operation temperature, T, close to the triple point of water, and comparison with the HITRAN database. Statistical uncertainties on the measured values correspond to a 68% confidence interval. Relative errors on the HITRAN data are in the range between 5% and 10%.

Spectroscopic parameter	Measured value at T	Rescaled value at T_0	HITRAN value
S ($\times 10^{-23}$ cm^2/molecule)	3.207 ± 0.003	3.001 ± 0.003	3.187
γ (cm^{-1}/atm)	0.4555 ± 0.0006	0.4289 ± 0.0006	0.480
δ (MHz/Torr)	-1.606 ± 0.005	-1.416 ± 0.005	

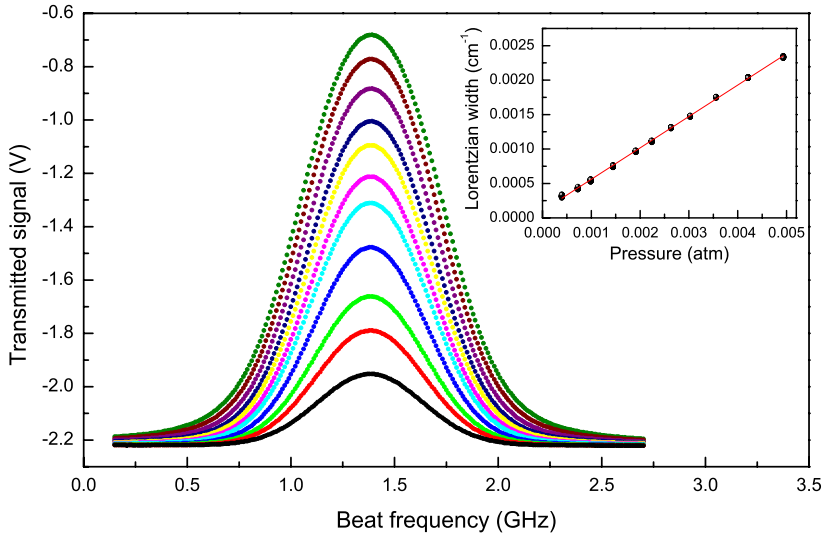

Fig. 6. Absorption lineshape at different $H_2{}^{18}O$ pressures. The inset shows the determination of the pressure broadening coefficient. Pressure values were properly corrected to take into account the thermal transpiration effect [16].

and shift coefficients (γ and δ), as well as the absolute linestrength (S), at the operation temperature T. In Fig. 6, examples of absorption profiles are reported, for $H_2{}^{18}O$ pressures between 40 and 500 Pa. The nonlinear least-squares analysis of these profiles yielded the integrated absorbance, the line center and the homogeneous width as a function of the gas pressure. Hence, as a result of a linear fit of each of the three data sets, the values of Table 1 were obtained, with a relative uncertainty varying between 0.1 and 0.3%, whose main contribution was given by the error in the measured pressures. The inset of Fig. 6 shows the linear fit of the homogeneous width versus the pressure data, showing a correlation coefficient of 0.99961. For a comparison with the HITRAN database [14], the linestrength and the pressure broadening coefficient were properly rescaled to retrieve their values at the reference temperature T_0 = 296 K, using the following equations [15]:

$$S(T_0) = S(T)\left(\frac{T}{T_0}\right)^{\frac{3}{2}} \exp\left[\frac{E''}{k_B}\left(\frac{1}{T}-\frac{1}{T_0}\right)\right] \quad (1)$$

#132562 - $15.00 USD Received 30 Jul 2010; revised 23 Sep 2010; accepted 23 Sep 2010; published 29 Sep 2010

$$\gamma(T_0) = \gamma(T)\left(\frac{T}{T_0}\right)^{0.75} \tag{2}$$

where E″ is the energy (in Joule) of the lower level involved in the ro-vibrational transitions and k_B is the Boltzmann constant. Concerning the S-parameter, a classical expression for the rotational partition function was assumed, while ignoring the temperature dependence of the vibrational partition function. As for the γ-parameter, the scaling equation, resulting from the elementary model of colliding hard spheres under the hypothesis of a dipole-dipole intermolecular potential, should have an exponent equal to 1. Here, we used a temperature dependence exponent of 0.75, as experimentally determined in Ref. 15. A similar equation holds also for the pressure shift coefficient, the exponent being 1.57 [15]. The last two columns of Table 1 clearly evidence a good agreement between the rescaled values and those of the HITRAN database, the deviations being well below the HITRAN uncertainties. It is worth noting that the pressure shift value does not agree with that recently obtained in the sub-Doppler regime, namely -0.93 MHz/Torr, at room temperature [10]. This slight discrepancy might be due to the different isotopic compositions of the employed water samples and to the different explored range of pressures. Furthermore, it can not be excluded the influence of the speed selection of the molecules that takes place when doing Lamb-dip spectroscopy.

4. Conclusion

High precision quantitative spectroscopy of $H_2{}^{18}O$ molecules at 1.38 μm has been demonstrated by means of a dual-laser absorption spectrometer based upon offset-frequency locking of a pair of extended cavity diode lasers. Such a system allows to perform highly accurate and reproducible frequency scans of the slave laser around a given vibration-rotation line. In a 3 - GHz wide scan, relative deviations from linearity were measured to be smaller than 4×10^{-6}, while the frequency stability over 300 successive scans was found to be better than 4×10^{-10}. These features, in conjunction to the extremely high linearity of InGaAs detectors [17], makes it possible to avoid any instrumental distortion in measuring absorption lineshapes, reaching an experimental accuracy limited only by the noise level. Moreover, for a further increase of the accuracy, spectra averaging is possible over an arbitrarily large number of acquisitions, provided that memory effects are reduced by means of a proper hydrophobic treatment of the cell walls. The spectrometer is presently being used for a spectroscopic determination of the Boltzmann constant, with improved accuracy as compared to previous experiments [7, 18]. In addition, the present work paves the way to new investigations on the departures of spectral lineshapes from the commonly used Voigt convolution, with the goal of achieving a clear discrimination between different collision processes responsible for these effects.

#132562 - $15.00 USD Received 30 Jul 2010; revised 23 Sep 2010; accepted 23 Sep 2010; published 29 Sep 2010